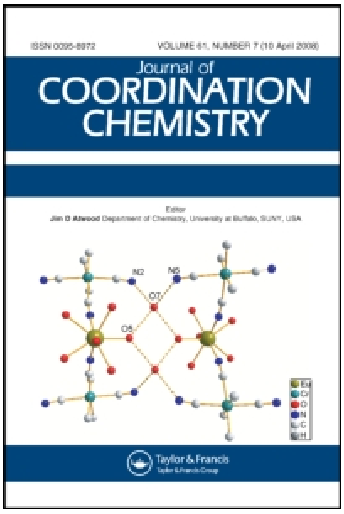

Journal of Coordination Chemistry

Publication details, including instructions for authors and subscription information:
http://www.informaworld.com/smpp/title~content=t713455674

Preparation, crystal structure, and physical characterization of a new hybrid material $(C_5H_9N_3)ZnCl_4 \cdot H_2O$

Sondra Walha[a]; Samia Yahyaoui[a]; Houcine Naili[a]; Tahar Mhiri[a]; Thierry Bataille[b]
[a] Faculté des Sciences de Sfax, Département de Chimie, Laboratoire de l'Etat Solide, Tunisie, France [b] Sciences Chimiques de Rennes (UMR CNRS 6226), Groupe Matériaux Inorganiques: Chimie Douce et Réactivité, Université de Rennes I, Avenue du Général Leclerc, 35042 Rennes CEDEX, France

To cite this Article Walha, Sondra , Yahyaoui, Samia , Naili, Houcine , Mhiri, Tahar and Bataille, Thierry(2010) 'Preparation, crystal structure, and physical characterization of a new hybrid material $(C_5H_9N_3)ZnCl_4 \cdot H_2O$', Journal of Coordination Chemistry, 63: 8, 1358 — 1368, First published on: 20 April 2010 (iFirst)

To link to this Article: DOI: 10.1080/00958971003782616

URL: http://dx.doi.org/10.1080/00958971003782616

Journal of Coordination Chemistry
Vol. 63, No. 8, 20 April 2010, 1358–1368

Preparation, crystal structure, and physical characterization of a new hybrid material $(C_5H_9N_3)ZnCl_4 \cdot H_2O$

SONDRA WALHA†, SAMIA YAHYAOUI*†, HOUCINE NAILI†,
TAHAR MHIRI† and THIERRY BATAILLE‡

†Faculté des Sciences de Sfax, Département de Chimie, Laboratoire de l'Etat Solide,
BP 1171, 3000 Sfax, Tunisie, France
‡Sciences Chimiques de Rennes (UMR CNRS 6226), Groupe Matériaux Inorganiques:
Chimie Douce et Réactivité, Université de Rennes I, Avenue du Général Leclerc,
35042 Rennes CEDEX, France

(*Received 28 October 2009; in final form 23 December 2009*)

An organic–inorganic hybrid compound $(C_5H_9N_3)ZnCl_4 \cdot H_2O$ was synthesized by slow evaporation and characterized by single-crystal X-ray diffraction, differential scanning calorimetry, thermogravimetry, temperature-dependent X-ray powder diffraction, infrared spectroscopy, and some preliminary theoretical calculations of non-linear optic activity. The compound crystallizes in the non-centrosymmetric space group $Pca2_1$ with unit cell parameters: $a = 22.714(5)$, $b = 7.313(5)$, $c = 7.301(5)$ Å, $Z = 4$, and $V = 1212.8(12)$ Å^3. The structure was solved using direct methods and refined by least-squares analysis [$R_1 = 0.0484$ and $wR_2 = 0.1255$]. It is built from isolated $[ZnCl_4]^{2-}$ anions, 2,5-diaminopyridinediium $[C_5H_9N_3]^{2+}$ cations, and water molecules which are connected by a 3-D hydrogen-bond network. Thermodiffractometry and thermogravimetric analyses indicate that its decomposition proceeds through four stages leading to a new crystalline anhydrous phases.

Keywords: Chemical preparation; Crystal structure; Thermal decomposition; Second-order NLO properties; IR spectroscopy

1. Introduction

Organic–inorganic hybrid solids A_2MX_4, in which A (or A_2) is an organic cation, M is a divalent metal ion, and X is a halide (Cl, Br), have been intensively investigated [1–3] due to their interesting properties [4–8] and potential applications including light emitting diodes, field-effect transistors and solar cells [9–12]. It is therefore vital to design and synthesize hybrid compounds and explore their various properties. Such complexes are characterized by strong intralayer covalent or ionic bonding in the organic frame and weak interlayer interaction such as van der Waals forces between the organic molecules. We report the synthesis and crystal structure of a new 2,5-diaminopyridinediium tetrachlorozincate(II) monohydrate, $(C_5H_9N_3)ZnCl_4 \cdot H_2O$,

---

*Corresponding author. Email: samia_yahyaoui@lycos.com

Journal of Coordination Chemistry
ISSN 0095-8972 print/ISSN 1029-0389 online © 2010 Taylor & Francis
DOI: 10.1080/00958971003782616

which has non-centrosymmetric arrangements and thus could possess non-linear optical (NLO) properties.

2. Experimental

2.1. *Material preparation*

Black plate crystals of $(C_5H_9N_3)ZnCl_4 \cdot H_2O$ were easily grown by slow evaporation at room temperature from aqueous solution of 2,5-diaminopyridine dihydrochloride $(C_5H_7N_3 \cdot 2HCl)$, zinc chloride $(ZnCl_2)$, and concentrated hydrochloric acid (HCl) with 1 : 2 : 1 molar ratio. The product was filtered off and washed with a small amount of distilled water.

2.2. *Single-crystal data collection and structure determination*

Single-crystal X-ray data of $(C_5H_9N_3)ZnCl_4 \cdot H_2O$ were collected at room temperature on a Nonius Kappa CCD diffractometer using Mo-Kα radiation ($\lambda = 0.71073$ Å) through the program COLLECT [12]. Corrections for Lorentz-polarization, peak integration, and background determination were carried out with the program DENZO [13]. Frame scaling and unit cell parameter refinement were performed with the program SCALEPACK [13]. Analytical absorption corrections were performed by modeling the crystal faces using NUMABS [14]. The crystal structure was determined in orthorhombic symmetry, space group is either *Pca2₁* or *Pcam*, from the appearance of the $(0kl)$ reflections with $l = 2n + 1$ and the $(h0l)$ reflections with $h = 2n + 1$ (n, integer). Therefore, first examination by assuming the centrosymmetric space group *Pcam* resulted in a high R_1 value of 0.14. Final examination by assuming the non-centrosymmetric space group $Pca2_1$ succeeded in the reduction of the R_1 value to 0.0484. On the other hand, ADDSYM analysis (PLATON [15]) revealed that the final structure model is pseudo-centrosymmetric. The large number of weak reflections that violate the reflection conditions of the *n* glide plane, the acentric intensity distribution, and the reasonable structure refinement indicate that $Pca2_1$ is the correct choice of space group. Zinc and chloride were located using direct methods with the program SHELXS-97 [16]. The oxygens and organic moiety were found from successive Fourier calculations using SHELXL-97 [17]. The water hydrogens were located in a difference Fourier map and refined with O–H distance of 0.86(1) Å and H–H distance restraints of 1.50(1) Å. Hydrogens bonded to C and N were geometrically positioned and allowed to ride on their parent atom, with C–H = 0.93 and N–H = 0.89 Å.

The nitrogens of pyridine are generally more basic than those of the amino groups. In this structure, it was very difficult to find a difference Fourier peak near the nitrogen of the pyridine ring that can be attributed to a proton. So we have considered only protonation of the two amino groups.

Crystallographic data and the results of the least-squares structure refinement are given in table 1. The final fractional atomic coordinates are given in the "Supplementary material". Bond distances and angles calculated from the final atomic coordinates, as well as probable hydrogen bonds, are listed in tables 2 and 3.

Table 1. Crystallographic data for $(C_5H_9N_3)ZnCl_4 \cdot H_2O$.

Empirical formula	$C_5H_{11}Cl_4N_3OZn$
Formula weight	336.34
Temperature (K)	293(2)
Wavelength (Mo-Kα) (Å)	0.71073
Crystal system	Orthorhombic
Space group	*Pca2₁*
Unit cell dimensions (Å)	
a	22.714(5)
b	7.313(5)
c	7.301(5)
Volume (Å^3), *Z*	1212.8(12), 4
Calculated density (g cm^{-3})	1.842
Absorption coefficient (mm^{-1})	2.879
F(000)	672
Crystal size (mm^3)	$0.467 \times 0.113 \times 0.026$
Habit-color	Plate-black
Secondary extinction coefficient	0.009(17)
θ range for data collection (°)	2.79–30.03
Limiting indices	$-30 \le h \le 31$; $-10 \le k \le 10$; $-10 \le l \le 10$
Unique data	3494
Max. and min. transmission	0.5296 and 0.9287
Refinement method	Full-matrix least-squares on F^2
Data/parameters	3008/136
Goodess-of-fit on F^2	1.021
Final *R* indices [$I > 2\sigma(I)$]	$R_1 = 0.0484$, $wR_2 = 0.1255$
Largest difference peak and hole (eÅ^{-3})	0.849 and -1.240

Table 2. Selected bond distances (Å) and angles (°).

Tetrahedron around Zn		Within the organic moiety	
Zn–Cl1	2.271(1)	N1–C4	1.460(5)
Zn–Cl2	2.291(2)	N2–C1	1.319(5)
Zn–Cl3	2.269(2)	N3–C1	1.350(5)
Zn–Cl4	2.258(2)	N3–C5	1.355(5)
Cl1–Zn–Cl2	109.57(4)	C1–C2	1.411(5)
Cl1–Zn–Cl3	108.23(5)	C3–C2	1.361(5)
Cl1–Zn–Cl4	108.54(7)	C3–C4	1.387(5)
Cl2–Zn–Cl3	106.44(7)	C4–C5	1.352(6)
Cl2–Zn–Cl4	109.46(4)	C1–N3–C5	123.8(3)
Cl3–Zn–Cl4	114.53(6)	N2–C1–N3	120.5(3)
		N2–C1–C2	122.7(3)
		N3–C1–C2	116.8(4)
		C2–C3–C4	119.6(3)
		C5–C4–C3	120.4(3)
		C5–C4–N1	120.4(4)
		C3–C4–N1	119.2(3)
		C3–C2–C1	118.9(4)

2.3. *Thermal analyzes*

Thermogravimetric analysis for $(C_5H_9N_3)ZnCl_4 \cdot H_2O$ was carried out with a Rigaku Thermoflex instrument. The 7.18 mg powdered sample was spread evenly in a large sample holder to avoid mass effects. The thermogravimetry (TG) run was performed in flowing air with a heating rate of 10°C min^{-1} from room temperature to 450°C.

Table 3. Hydrogen-bonding geometry (Å, °).

D–H···A	d(D–H) (Å)	d(H···A) (Å)	d(D···A) (Å)	∠D–H···A (°)
N1–H1B···O	0.89	2.09	2.861(6)	144.5
N1–H1C···O^{I}	0.89	2.41	3.190(6)	146.0
N1–H1A···Cl3	0.89	2.65	3.516(4)	164.8
N1–H1B···Cl2	0.89	2.86	3.309(5)	112.5
N1–H1C···$Cl4^{II}$	0.89	2.87	3.297(4)	110.9
N2–H2A···$Cl1^{III}$	0.89	2.53	3.358(4)	115.6
N2–H2B···$Cl2^{IV}$	0.89	2.82	3.355(4)	119.7
O–HW1···$Cl3^{V}$	0.96(2)	2.48(13)	3.187(4)	130(13)
O–HW2···$Cl2^{VI}$	0.95(2)	2.40(5)	3.212(4)	142(6)

Symmetry codes: $^{I}-x, -y+2, z+1/2$; $^{II}x, y, z+1$; $^{III}x, y+1, z+1$; $^{IV}-x+1/2, y, z+1/2$; $^{V}x, y+1, z$; and $^{VI}-x, -y+2, z+1/2$.

Temperature-dependent X-ray diffraction (TDXD) was performed with a D5005 powder diffractometer (Bruker AXS) using Cu-Kα radiation [$\lambda(K\alpha_1) = 1.5406$ Å, $\lambda(K\alpha_2) = 1.5444$ Å] selected with a diffracted-beam graphite monochromator, and equipped with an Anton Paar HTK1200 high-temperature oven camera.

The differential scanning calorimetry (DSC) at high temperature was performed with a SETARAM DSC131 instrument for temperatures ranging from 20°C to 400°C at a rate of 10°C min^{-1}. A polycrystalline sample of 22.08 mg was placed in a hermetic aluminum cell in nitrogen atmosphere.

2.4. *IR spectroscopy*

IR measurements were obtained using a Perkin Elmer 1600 FT spectrometer. Samples were diluted with spectroscopic KBr and pressed into a pellet. Scans were run over the range of 400–4000 cm^{-1}.

3. Results

3.1. *Crystal structure of* $(C_5H_9N_3)ZnCl_4 \cdot H_2O$

The asymmetric unit contains one $[ZnCl_4]^{2-}$, one 2,5-diaminopyridinediium, and one uncoordinated water molecule (figure 1). The 2,5-diaminopyridinediium tetrachlorozincate(II) monohydrate obtained here crystallizes in the non-centrosymmetric space group *Pca2₁*. It consists of inorganic entities, $[ZnCl_4]^{2-}$, organic moieties of $(C_5H_9N_3)^{2+}$, and uncoordinated water molecule, forming mixed organic–inorganic layers in (*b*, *c*) planes. These layers are stabilized and interconnected by three types of hydrogen bonds, N–H···Cl, N–H···O, and O–HW···Cl (figure 2).

The $ZnCl_4$ tetrahedron (figure 1) is slightly irregular as seen in other analogous compounds [18, 19]. Zn–Cl distances range from 2.285(2) to 2.291(2) Å and the Cl–Zn–Cl angles vary from 106.4(7) to 114.5(6)° (table 2). The mean Zn–Cl distance is 2.272 Å, in agreement with that calculated from the bond valence program VALENCE [20] for a four-fold chloride-coordinated Zn^{II}, 2.285 Å. Zinc atoms are stacked one over the other along the three crystallographic axes and are isolated from

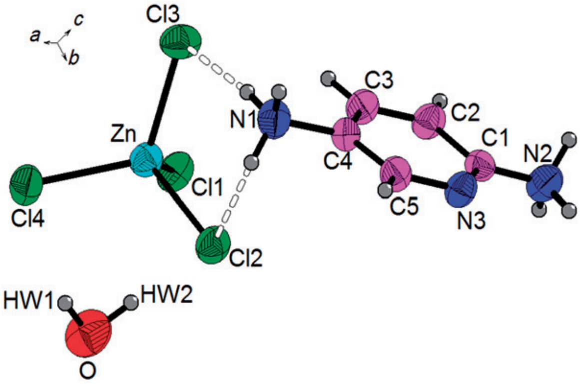

Figure 1. Part of the crystal structure of the title compound showing the asymmetric unit and atom numbering. Displacement ellipsoids are drawn at the 50% probability level.

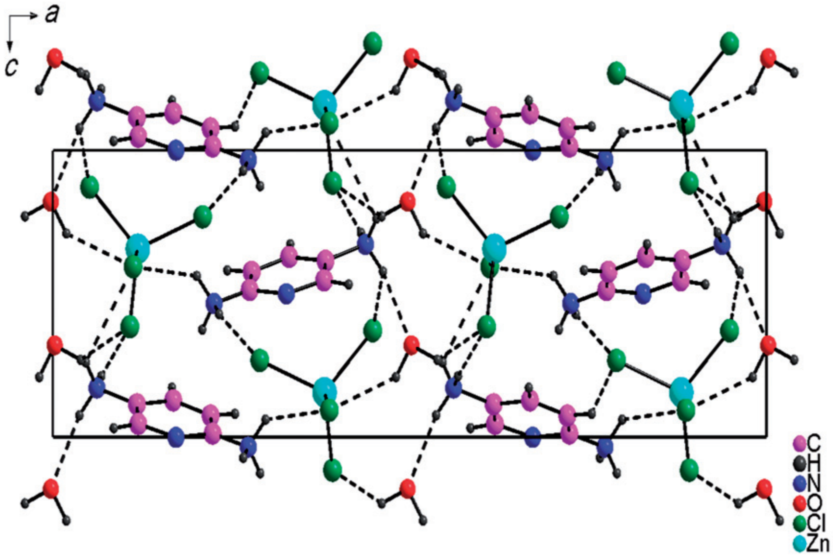

Figure 2. Projection of the crystal structure of $(C_5H_9N_3)ZnCl_4 \cdot H_2O$ along the *b*-axis. Bonds are shown as dashed lines (as in the following figures).

each other with a shortest distance Zn–Zn = 6.522(15) Å. The $ZnCl_4$ tetrahedra are linked to water molecules into zig-zag chains by O–HW $\cdots$ Cl hydrogen bonds along the *c* direction, as illustrated in figure 3. Within the weak O–HW $\cdots$ Cl intermolecular H-bonds, the O $\cdots$ Cl distances range from 3.187(4) to 3.212(4) Å and the O–HW–Cl angles are between 130(13) and 142(6)° (table 4). All chlorides of $ZnCl_4$ are involved in hydrogen bonds with the ammonium groups of surrounding organic cations, each acting as an acceptor of one (Cl1, Cl3, and Cl4) or two (Cl2) hydrogen bonds (figure 4). The N–H $\cdots$ Cl hydrogen bonds link organic cations and inorganic anions to give mixed organic–inorganic layers (9.66 Å) parallel to the *ac* plane (figure 2). The interlayer space

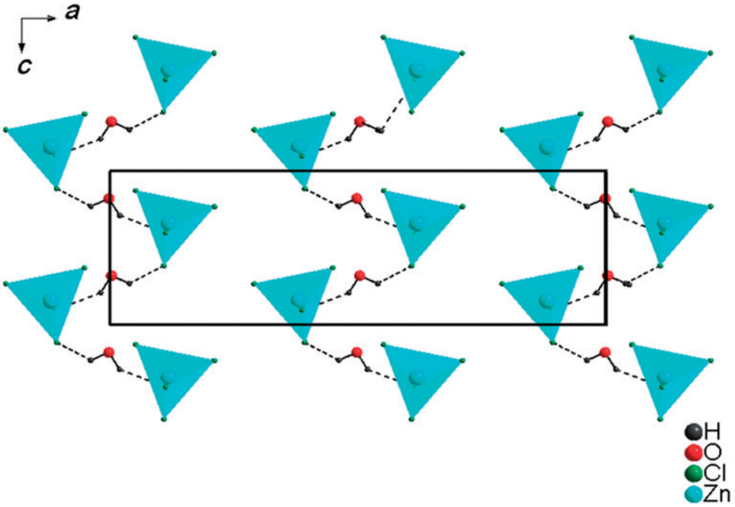

Figure 3. Zig-zag chains formed by the association of $ZnCl_4$ and H_2O by O–HW···Cl hydrogen bonds along the *c*-axis.

Table 4. Dihedral angles of the 2,5-diaminopyridinediium.

Orientations (*i*–*j*)	Dihedral angles (°)
A–B	15.1(1)
A–C	39.6(1)
A–D	42.6(1)
B–D	42.6(1)
B–C	39.6(1)
C–D	15.1(1)

thickness is 1.69 Å. The negative charges of the inorganic part are compensated by 2,5-diaminopyridinediium cations which are located in general positions. The C–N and C–C distances of 1.371(6) and 1.377(6) Å, respectively, are close to the values observed in homologous derivatives [21, 22]. The organic entity $[C_5H_9N_3]^{2+}$ adopts four possible orientations in the *ac* plane generating six dihedral angles (figure 5 and table 4). Figure 6 shows that each organic cation has hydrogens bonded to nitrogen in N–H···O and N–H···Cl hydrogen bonds, connecting with four $ZnCl_4$ tetrahedra and two water molecules. The N–H···O hydrogen bonds vary from 2.861(6) to 3.190(4) Å and the N–H–O angles range between 144.5 and 146.0° (table 3). The water molecules are located above and below the layers and connect them *via* hydrogen bonds (figure 2), participating in two types of hydrogen bonds O–H···Cl and N–H···O as a donor or an acceptor, respectively (figure 7 and table 3), playing an important role in cohesion of the structure.

The presence of the aromatic ring is confirmed using IR spectroscopy with C–C and C–N stretches measured at 1678 and 1468 cm^{-1}, respectively. Bands in the range 3322–2924 cm^{-1} and 1636–1502 cm^{-1} are NH_3^+ stretching and bending vibrations, respectively. These data are in agreement with double protonation of the organic moiety.

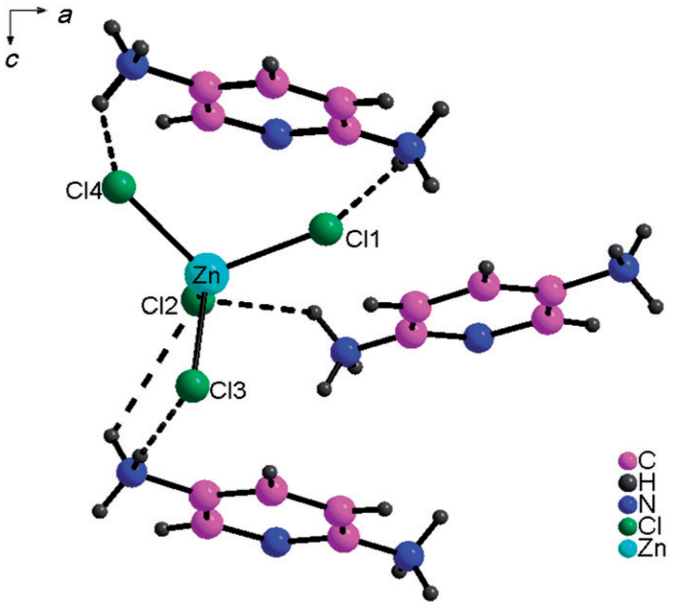

Figure 4. Neighboring chlorides in the Zn(II) tetrahedron in $(C_5H_9N_3)ZnCl_4 \cdot H_2O$.

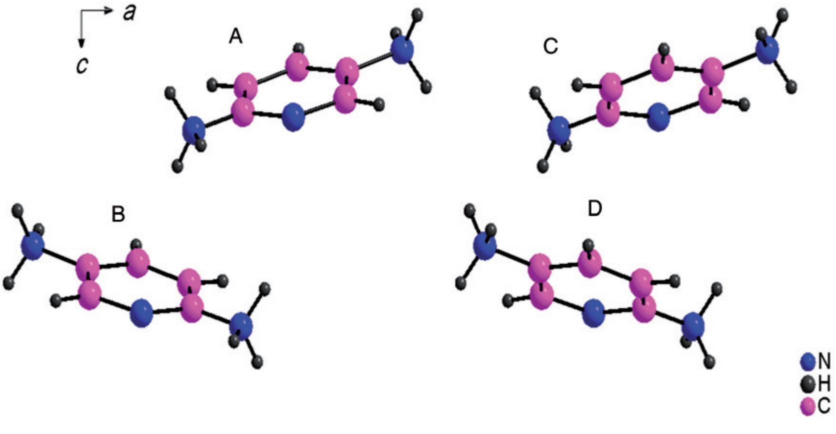

Figure 5. Dihedral angles of 2,5-diaminopyridinediium.

3.2. *Thermal behavior of the precursors*

Successive powder patterns obtained during the thermal decomposition of $(C_5H_9N_3)ZnCl_4 \cdot H_2O$ in air in the temperature range of 20°C–870°C are provided as the "Supplementary material". The TG and DSC were carried out with a heating rate of $10°C\,min^{-1}$ between 25°C and 450°C (Supplementary material). The first transformation occurs from 55°C to 120°C with a weight loss of 5.47% in agreement with a loss of one water molecule (Calcd weight loss of 5.35%), thus leading to the first crystalline

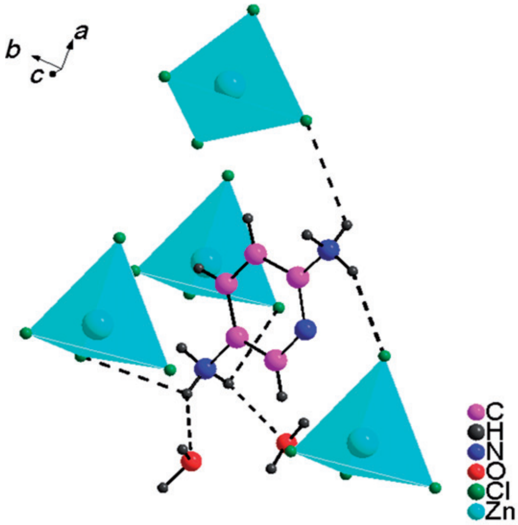

Figure 6. The coordination environment of $(C_5H_9N_3)^{2+}$.

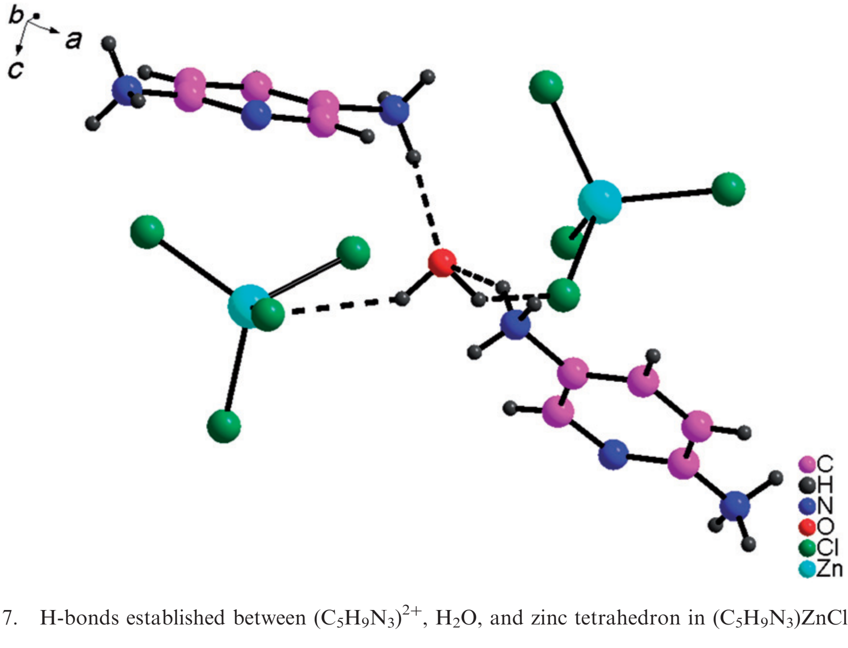

Figure 7. H-bonds established between $(C_5H_9N_3)^{2+}$, H_2O, and zinc tetrahedron in $(C_5H_9N_3)ZnCl_4 \cdot H_2O$.

anhydrous phase α-$(C_5H_9N_3)ZnCl_4$. This is accompanied with an endothermic peak on the DCS curve, maximum at 80°C. At 120°C, some diffraction lines emerge from the background, indicating the second anhydrous phase β-$(C_5H_9N_3)ZnCl_4$. The formation of this phase is accompanied by an endothermic peak at 110°C, as depicted by the DSC curve. The next transformation starts at 210°C and corresponds to the decomposition

Table 5. Comparison of calculated molecular hyperpolarizabilities.

Entity	λ_{max} (nm)	Hyperpolarizability β
$(C_5H_9N_3)^{2+}$	0	0.10
	1907	0.11
	1064	0.15
$(C_5H_9N_3)ZnCl_4$	0	0.71
	1907	0.84
	1064	1.44

of the amine, accompanied with a strong endothermic peak on the DSC curve at 220°C. The last transformation starts at about 380°C on the TDXD plot. Interrogation of the International Center for Diffraction Data (ICDD) powder diffraction file [23] revealed that this phase corresponds to the formation of zinc oxide.

3.3. *NLO properties*

The method that we have chosen to determine the first hyperpolarizability of 2,5-diaminopyridinediium tetrachlorozincate(II) monohydrate is based on ZINDO method in conjunction with SOS formalism [24, 25]. ZINDO method has advantages over the electric-field-induced second harmonic generation; it has been demonstrated as a useful and simple method to characterize the β values. The first hyperpolarizabilities β for the organic entity $(C_5H_9N_3)^{2+}$ and $(C_5H_9N_3)ZnCl_4$ are listed in table 5 for some wavelengths. These calculations show a clear dependence between β and the relative positions of the organic and the inorganic moieties. Indeed, β values of $(C_5H_9N_3)ZnCl_4$ are larger than that of the amine entity $(C_5H_9N_3)^{2+}$. However, in these two cases these values are weak by comparison with other materials [26] having large second-order NLO responses. This result seems to be logical because the shortest distance between the organic and the inorganic moieties is 2.53(1) Å, leading to a weak charge transfer between these two entities.

4. Concluding remarks

The single-crystal structure, thermal decomposition, and some theoretical NLO calculations of an organic–inorganic hybrid $(C_5H_9N_3)ZnCl_4 \cdot H_2O$ are reported. The X-ray examination demonstrates that it crystallizes in the non-centrosymmetric space group *Pca2₁* at room temperature with the structure built from isolated ions: $[C_5H_9N_3]^{2+}$, $(ZnCl_4)^{2-}$, and water molecule linked by hydrogen bonds. The thermal behavior of this material, studied by TG, TDXD, and DSC shows that the decomposition proceeds through four steps: the loss of water molecule leading to α-$(C_5H_9N_3)ZnCl_4$, formation of the second anhydrous phase β-$(C_5H_9N_3)ZnCl_4$, decomposition of the organic entity, and finally the formation of zinc oxide. Study of the NLO properties of this material, using theoretical calculations, shows weak β values.

Ferroelectric tetrachlorozincate compounds can be obtained by using non-centrosymmetric protonated amine cations. Indeed, a ferroelectric tetramethylammonium tetrachlorozincate, $[N(CH_3)_4]_2[ZnCl_4]$, and space group $P2_1cn$, has been observed as a transition phase in a narrow temperature range of 3 K [27]. In this study, the acentric crystal structure of the title compound was expected from the non-centrosymmetric character of the organic 2,5-diaminopyridinediium used in the synthesis. The extended use of acentric organic molecules would allow us to obtain new ferroelectrics at room temperature, stable within a wider temperature range. Therefore, it is of interest to investigate further the synthesis of such salts by using non-centrosymmetric diamine molecules [28].

Supplementary material

CCDC 738540 contains the supplementary crystallographic data for **1**. These data can be obtained free of charge *via* http://www.ccdc.cam.ac.uk/conts/retrieving.html, or from the Cambridge Crystallographic Data Centre, 12 Union Road, Cambridge CB2 1EZ, UK; Fax: +44-1223-336033; or Email: deposit@ccdc.cam.ac.uk.

Acknowledgments

We are grateful to Dr Thierry Roisnel (Centre de Diffractométrie X, Sciences Chimiques de Rennes, Université de Rennes I) and M. Gérard Marsolier for supplying the single-crystal and powder X-ray diffraction data collection and Dr Pascal G. Lacroix (Université de Toulouse) for the NLO theoretical calculations.

References

[1] C.-X. Cai, L. Xu, Y.-Q. Tian, X.-Z. You. *Acta Crystallogr.*, **E58**, m399 (2002).
[2] A. Elangovan, A. Thamaraichelvan, A. Ramu, S. Athimoolam, S. Natarajan. *Acta Crystallogr.*, **E63**, m201 (2007).
[3] H. Zhang, L. Fang, R. Yuan. *Acta Crystallogr.*, **E61**, m609 (2005).
[4] D.B. Mitzi, C.A. Field, W.T.A. Harrison, A.M. Guloy. *Nature*, **369**, 467 (1994).
[5] P. Day. *Philos. Trans. R. Soc. London, Ser. A*, **314**, 145 (1985).
[6] D.B. Mitzi, S. Wang, C.A. Field, C.A. Chess, A.M. Guloy. *Science*, **267**, 1473 (1995).
[7] G.C. Papavassiliou. *Prog. Solid State Chem.*, **25**, 125 (1997).
[8] B. Tieke, G. Wegner. *Angew. Chem. Int. Ed. Engl.*, **20**, 687 (1984).
[9] G.C. Papavassiliou, I.B. Koutselas, A. Terzis, M.H. Whangbo. *Solid State Commun.*, **96**, 695 (1994).
[10] J.G. Bednorz, K.A. Mueller. *Z. Phys. B*, **64**, 189 (1986).
[11] A.J. Millis, I. Shraian, R. Mueller. *Phys. Rev. Lett.*, **77**, 175 (1996).
[12] Nonius, *Kappa CCD Program Software*, Nonius BV, Delft, The Netherlands (1998).
[13] Z. Otwinowski, W. Minor, C.W. Carter, R.M. Sweet (Eds.). *Methods in Enzymology*, Vol. 276, Academic Press, New York (1997).
[14] J. de Meulenaer, H. Tompa. *Acta Crystallogr.*, **19**, 1014 (1965).
[15] A.L. Spek. *PLATON, A Multipurpose Crystallographic Tool*, Utrecht University, The Netherlands (2001).
[16] G.M. Sheldrick. *SHELXS 97-Programs for Crystal Solution*, University of Göttingen, Göttingen, Germany (1997).

[17] G.M. Sheldrick. *SHELXL 97-Programs for Crystal Structure Refinement*, University of Göttingen, Göttingen, Germany (1997).
[18] A. Fowkes, W.T.A. Harrison. *Acta Crystallogr.*, **E60**, m59 (2004).
[19] M. Rademeyer. *Acta Crystallogr.*, **E61**, m304 (2005).
[20] I.D. Brown. *J. Appl. Crystallogr.*, **29**, 479 (1996).
[21] A. Kanazawa, T. Ikeda, Y. Nagase. *Chem. Mater.*, **12**, 3776 (2000).
[22] I.A. Morkan, K. Guven, S. Ozkar. *J. Organomet. Chem.*, **689**, 2319 (2004).
[23] International Centre for Diffraction Data (ICCD), 12 Campus Boulevard Newtown Square, PA, USA (2002).
[24] J. Ridley, M.C. Zerner. *Theor. Chim. Acta*, **32**, 111 (1973).
[25] J. Ridley, M.C. Zerner. *J. Mol. Spectrosc.*, **50**, 457 (1974).
[26] P.L. Franzen, S.C. Zilio, A.E.H. Machado, J.M. Madurro, A.G. Brito-Madurro, L.T. Ueno, R.N. Sampaio, N.M. Barbosa Neto. *J. Mol. Struct.*, **892**, 258 (2008).
[27] G. Madariaga, F.J. Zuniga, J.M. Perez-Mato, M.J. Tello. *Acta Crystallogr.*, **B43**, 356 (1987).
[28] S. Walha, S. Yahyaoui, H. Naili, T. Mhiri, T. Bataille, in preparation.